

Engineered Recombinant Factor VII Q²¹⁷ Variants with Altered Inhibitor Specificities[†]

Yu-Jia Chang,[‡] Nobuko Hamaguchi,[§] Shu-Chuan Chang,[‡] Wolfram Ruf,^{||} Ming-Ching Shen,[‡] and Shu-Wha Lin^{*‡}

Graduate Institute of Medical Technology and Department of Laboratory of Medical Sciences, College of Medicine, National Taiwan University, Taiwan, ROC, Brandeis University, Rosenstiel Center, Waltham, Massachusetts 02454, and Department of Immunology, The Scripps Research Institute, La Jolla, California 92037

Received January 8, 1999; Revised Manuscript Received June 7, 1999

ABSTRACT: Recombinant factor VII with residue 217 (chymotrypsinogen numbering system) converted to alanine (VIIQ217A), glutamic acid (VIIQ217E), or glycine (VIIQ217G) was characterized. In a prothrombin time assay, VIIQ217E demonstrated 100%, VIIQ217A 15%, and VIIQ217G <1% clotting activities relative to wild-type VII. Binding of VIIQ217A and VIIQ217G to TF was comparable to that of wild-type VII to TF. All the variants were readily activated by factor Xa. Autoactivation in the presence of TF was efficient with VIIQ217E, slow with VIIQ217A, but undetected with VIIQ217G. Relative to wild-type VII added at the same concentration, VIIQ217E had no effect on the PT of normal plasma, whereas VIIQ217A slightly and VIIQ217G dramatically prolonged the clotting time in a dose-dependent manner. Activation of macromolecular substrates paralleled this functional inhibition. The k_{cat}/K_M values for factor X activation in the presence of TF were 2.4 for VIIaQ217E as compared to 1.9 ($\text{M}^{-1} \text{s}^{-1} \times 10^7$) for wild-type VIIa, 1.57 for VIIaQ217A, and 0.05 with VIIaQ217G. In comparison to wild-type VIIa, VIIaQ217E cleaved the chromogenic substrate S2765 (Z-D-Arg-Gly-Arg-pNA) with 10-fold higher k_{cat} . Analysis of the interactions with the inhibitors TFPI and antithrombin III demonstrated that VIIaQ217A but not VIIaQ217E or VIIaQ217G was inhibited less efficiently by TFPI either in the presence or in the absence of factor Xa. In contrast, VIIaQ217A association with antithrombin III in the presence of heparin was the fastest among the variants with a second-order rate constant of $2.31 (\times 10^3 \text{ M}^{-1} \text{ min}^{-1})$, as compared to 0.47 and 1.47 for VIIaQ217E and wild-type VIIa, respectively. Our results demonstrate that residue Q²¹⁷ is important in regulating substrate and, more importantly, inhibitor recognition by VIIa.

Blood coagulation is initiated when circulating factor VII (or factor VIIa) binds to the cell surface, transmembrane protein, tissue factor (TF), on the cell surface and forms a catalytic complex (VIIa–TF)¹ capable of activating factors IX and X (1). The gene of human factor VII is 12.8 kb which codes for a protein precursor with a preproleader peptide of 60 or 38 amino acids and a mature secreted zymogen of 406 amino acids (2, 3). The structural modules of the amino-terminal light chain are a γ -carboxyglutamic acid (Gla)

domain and two epidermal growth factor (EGF)-like modules, followed by the carboxy-terminal heavy chain that is a trypsin-like protease domain (1). Activated VII (VIIa) is generated by hydrolysis of the Arg¹⁵²–Ile¹⁵³ bond to become a disulfide-bonded two-chain molecule. Several enzymes are capable of activating factor VII, including factor Xa (4–6), factor IXa (6, 7), factor XIIa (8, 9), thrombin, and the VIIa–TF complex (10–12). VIIa's enzymatic activity is greatly enhanced by its association with TF (10, 11, 13, 14). The critical residues for the interaction of VIIa with TF have been mapped by site-directed mutagenesis (14–17), which was in good agreement with the crystal structure of the VIIa–TF complex (18). Each of the structural modules of VIIa makes contacts with the receptor and cofactor TF.

VIIa circulates in plasma (19). Factor IXa was proposed to contribute to the levels of VIIa in plasma, because hemophilia B, but not hemophilia A, patients had reduced levels of circulating VIIa (20). When bound to TF, VII is rapidly activated to VIIa by factor Xa, indicating an early amplification step in the initiation of coagulation (4, 5). VIIa–TF's enzymatic activity is regulated by tissue factor pathway inhibitor (TFPI) (21–24), Kunitz-type inhibitor which in part circulates in association with plasma lipoproteins (21). In the presence of factor Xa, TFPI inactivates VIIa efficiently by forming a quaternary complex of VIIa–TF–TFPI–Xa in which the catalytic sites of factors Xa and

[†] This work was supported by grants from the Department of Health on Taiwan (DOH85-HR-521 and DOH86-HR-521) and from the National Science Council, Taiwan (NSC84-2732-B002-003 and -004, NSC85-2331-B002-213M02).

* Address proofs to this author at the Graduate Institute of Medical Technology, National Taiwan University, College of Medicine, No. 1, Chang-Te Street, Taipei, Taiwan, ROC. Telephone: 886-2-23970800, ext 6907. Fax: 886-2-23817083. Email: mtshuwha@ccms.ntu.edu.tw.

[‡] National Taiwan University.

[§] Brandeis University.

^{||} The Scripps Research Institute.

¹ Abbreviations: ATIII, antithrombin III; VII, factor VII; VIIQ217A, VIIQ217E, and VIIQ217G, glutamine at residue 217 replaced by alanine, glutamic acid, and glycine, respectively; TFPI, tissue factor pathway inhibitor; PCPS, phosphatidylcholine and phosphatidylserine; ITS, insulin–transferrin–sodium selenite; RT-PCR, reverse transcription–polymerase chain reaction; SDS–PAGE, sodium dodecyl sulfate/polyacrylamide gel electrophoresis; FFR–chloromethyl ketone, Phe–Phe–Arg–chloromethyl ketone.

VIIa are inactivated by occupancy with a Kunitz-type inhibitor module of TFPI (19). However, at high concentrations, TFPI is capable of inhibiting VIIa-TF's activity in the absence of factor Xa (25, 26). VIIa-TF may also be inhibited by antithrombin III (ATIII) in the presence of heparin (27–29). ATIII is present in plasma at a higher concentration than TFPI and may thus serve as the initial inhibitor of VIIa-TF. However, binding of ATIII induces dissociation of VIIa from TF (30), indicating that the more stable complex of VIIa-TF with TFPI may account for more prolonged down-regulation of TF function *in vivo*.

Recombinant VIIa is used as bypass therapy for management of hemophilia A patients with inhibitors to factor VIII (31). Moreover, recombinant proteins are ideal tools for assessing protein functions, and they provide new therapeutic strategies. For example, engineered thrombin variants created by alanine scanning mutagenesis have provided novel protein molecules with altered preferences for substrates and/or inhibitors (32). A single amino acid substitution of E²¹⁷ (chymotrypsin numbering, 229 in thrombin numbering system) by alanine drastically converts thrombin from a procoagulant into an anticoagulant enzyme (33). Multiple amino acid replacements at this position resulted in the identification of a thrombin molecule (thrombin E229K) with optimized specificities as an anticoagulant (34). Moreover, E²¹⁷ in thrombin forms a salt bridge with R221. This salt bridge is considered critical for the conformational link to a single Na⁺ site in thrombin that regulates substrate specificity (35). E²¹⁷ is conserved among thrombin, protein C, factor X, factor IX, and bovine factor VII. However, in human VII, Q is substituted for E. The functional consequences of mutations at the Q²¹⁷ position of factor VII were investigated in this study. Three variants with replacement of Q²¹⁷ (Q³⁶⁶ in the mature VII protein) by A, E, and G have been generated and characterized regarding their interaction with TF, factors IX and X, and two different inhibitors, TFPI and ATIII.

EXPERIMENTAL PROCEDURES

Materials. All the restriction endonucleases and polymerases were obtained from New England Biolabs, Inc. (Beverly, MA). Geneticin (G418) was from Gibco BRL (Gaithersburg, MD). QAE-Sephadex was from Pharmacia (Sweden). VII-deficient plasma, ATIII, and phosphatidylcholine (PC) and phosphatidylserine (PS) were purchased from Sigma Chemical Co. (St. Louis, MO). The concentration of ATIII was calculated as described (28). Human factor XIa, plasma-derived VIIa, and factor X were obtained from Enzyme Research Laboratory (South Bend, IN). sTF was prepared as described (36). TFPI was a gift from Dr. Yuichi Kamikubo (Kaketsuken, Kyokushi Kikuchi, Kumamoto 869-1298, Japan). Spectrozyme FXa and recombinant human TF were purchased from American Diagnostica (Greenwich, CT). S-2288 and S2765 were products of Chromogenix (Sweden). Chromozyme tPA and ITS (insulin–transferrin–sodium selenite) were from Boehringer Mannheim (Germany). Z-Arg-ONb was a gift of Dr. Iwanaga (37). Monoclonal antibody F5-8A1 against the light chain of human VII was as described (16). Another antibody, 231-7, to the first EGF-like domain of human VII (38), was a gift from Dr. Blajchman (Department of Pathology, McMaster University, Canada).

Cloning, Mutagenesis, and Transfection. A 1.5 kb human VII cDNA was obtained by RT-PCR amplification of RNA from normal liver tissues using two oligonucleotide primers, 5'-CAGCGGATCCACCATTTTCATCATGGTCTCCGAGGCCCTCAGG-3' and 5'-cattggatcctctaccaccataactg-3'. Reaction conditions were as described previously (39). This fragment was sequenced to confirm its identity to the published sequence of human VII. *In vitro* mutagenesis was performed as described (40) using three oligonucleotides [5'-TCGTCAGCTGGGGCG(C or A or G)GGGATGCGCAACCGTGG-3'] to generate the VII mutants VIIQ217A, VIIQ217E, or VIIQ217G. After confirmation by sequencing, wild-type and mutated VII cDNAs were subcloned into pCMV5 and expressed by transfection into human 293 cells (41). Cell culture conditions were essentially as described previously (40). Transfection was performed by electroporating 10⁷ cells with 20 µg of DNA and 2 µg of pSV2neo at 350 V and 250 µF (Gene Pulser II, Bio-Rad) followed by selection in medium containing G418 (0.6 mg/mL). Surviving clones were identified immunologically by ELISA and expanded in serum-free medium supplemented with ITS (10 µg/mL) and vitamin K (10 µg/mL).

Purification of VII. Purification of VII was conducted by chromatography on QAE Sephadex A-50. The cultured media were centrifuged at 4000g for 30 min and loaded onto columns equilibrated with 20 mM Tris-HCl, pH 8.5, and 150 mM NaCl, 5 mM EDTA, and 5 mM benzamidine at a flow rate of 1 mL/min. After the column was washed with 20 mM Tris-HCl, pH 7.5, 100 mM NaCl (TBS)/benzamidine, elution was performed with 20 mM Tris-HCl, pH 8.5, 150 mM NaCl plus 5 mM CaCl₂. VII-containing fractions were identified by ELISA using F5-8A1 and peroxidase-labeled 231/7 prepared following manufacturer's instructions (Pierce, Rockford, IL). Purified proteins were collected, dialyzed against the appropriate buffer (to reach 20 mM Tris-HCl, pH 7.5, and 100 mM NaCl after reconstitution), and lyophilized. The protein concentration was also measured by a protein assay kit (Bio-Rad) modified from the Bradford method (42).

Phospholipid Vesicles and Relipidation of Recombinant TF. Preparation of phospholipids followed the procedures described by Szoka and Papahadjopoulos (43). To generate PCPS 75%/25% vesicles, 7.5 mg of PC and 2.5 mg of PS were dissolved in chloroform, evaporated in N₂ gas, and redissolved in cyclohexane. The PCPS mixtures were then vacuum-dried for 20 h using a rotor evaporator and subsequently resuspended at 4 °C overnight in 2.5 mL of TBS plus 0.1 mM EDTA (pH 8.0) to generate a lipid emulsion. The emulsion was further sonicated and fractionated at 50 000 rpm for 30 min using Ti-60 rotor (Beckman), and the supernatant was collected and used. The phospholipid content of the vesicles was determined by color development in ferrothiocyanate (44). Preparation of relipidated TF followed the procedure of Zhong et al. (45) by mixing 100 µL of full-length TF (2.5 µg) and an equal volume of PCPS. The final concentration of TF is 156 nM, and that of PCPS is 1 mM. The activity was determined by PT, and at a 1:40 dilution, the clotting time was about 15–20 s (45).

Activation by Factor Xa and Autoactivation in the Presence of TF. Activation by factor Xa was conducted by incubating 1 µg of the mutant and wild-type VII with 1/500 (w/w) of the enzyme in TBS and 5 mM CaCl₂ (TBS/Ca)

and 100 μ M PCPS at 37 °C for 60 min. Aliquots of the reaction mixtures were withdrawn at timed intervals and analyzed by SDS–polyacrylamide gel electrophoresis (SDS–PAGE) with a 10–15% acrylamide gradient (40) followed by silver staining. Autoactivation of the VII mutants in the presence of TF was performed by incubating 1 μ M proteins with 10 nM relipidated TF at 37 °C for 0–3 h before aliquots were analyzed as described above.

Clotting Assay and TF Binding. One-stage prothrombin time (PT) assays were performed as described (40) using VII-deficient plasma and a commercially-available thromboplastin extract (Thromborel S, Behring, Germany). When competition of the mutants with normal VII was evaluated by PT assays, 0.1 mL of various amounts (0–10 μ g/mL) of purified mutant proteins was incubated with an equal volume of normal-pooled plasma at 37 °C for 3 min. The clotting time was initiated by adding 0.2 mL of thromboplastin. The ability of mutant or wild-type proteins to influence PT was determined by plotting the clotting time vs the amount of the proteins added on a log/log scaled axis. Binding of wild-type and mutant VII (and VIIa) to TF was analyzed by the surface plasmon resonance method using BIAcore 2000 (Pharmacia Biosensor AB) as described previously (16).

Enzymatic Activities. The amidolytic activities of the VIIa mutants were measured in a microtiter plate format (Molecular Devices Corp.) by incubating 10 nM activated proteins (generated by bovine factor Xa at concentrations not interfering with the experiments) and 10 nM sTF with a 0.1–1 mM sample of the chromogenic substrates at 37 °C in 100 μ L of TBS plus 0.1% BSA. The change of absorbance at 405 nm was recorded, and the kinetic parameters, K_M and k_{cat} , were calculated by the Lineweaver–Burk plot. Activation of factor X (and factor IX) was performed using 2 nM VIIa, 3 nM relipidated TF (containing 60 μ M PCPS), and 0.4 μ M factor X (or 0.5 μ M factor IX) in TBS/Ca with PCPS to a final concentration of 100 μ M. The generated products were analyzed by SDS–PAGE.

Kinetic values for activation of factor X by mutant VIIa's were derived as described (46) with minor modifications. Briefly, when activation of factor X in the absence of TF was performed, 20 nM wild-type or mutant VIIa was incubated with factor X (0–4 μ M) and 300 μ M S2222 in a total volume of 100 μ L of TBSA/Ca plus 0.1% BSA and 100 μ M PCPS. The change of absorbance at 405 nm was monitored for 3.5 h. The absorbance of the initial rate of factor X activation mediated by wild-type and mutant factor VIIa was converted to molar Xa per minute by the equation:

$$\text{absorbance } (A_{405}) = at^2 + bt + c$$

where “ a ” reflects the rate at which factor Xa cleaves the chromogenic substrate and the rate at which factor X is cleaved by wild-type and mutant factor VIIa–PCPS complex, “ b ” is the amount of factor Xa present in zymogen factor X, and “ c ” is the amount of cleaved substrate at time 0.

When activation was in the presence of TF, 0.5 nM VIIa was incubated with a 10-fold molar excess of relipidated TF (5 nM) at ambient temperature for 20 min in a total volume of 30 μ L of TBS/Ca/PCPS plus 0.1% BSA. Factor X (0.06–2.4 μ M) was then added to initiate the reaction at 37 °C. The final volume of the reaction mixture was 60 μ L, and

final concentrations were 0.3 nM for wild-type and mutant VIIa, 30 nM for relipidated TF, and 130 μ M for PCPS. At 5 and 20 min after incubation, an appropriate amount of the mixture was withdrawn and stopped by adding 5 times excess volume of quenching buffer (20 mM MES, pH 5.8, 20 mM EDTA, and 8% Lubrol-PX) and 4 times excess of neutralization buffer (25 mM EDTA and 0.2 M MOPS, pH 8.8). The amount of factor Xa generated was quantitated by adding S2222 (0.3 mM) and following the absorbance change at 405 nm. The rates of S2222 hydrolysis were converted to moles per liter of factor Xa by comparison to a standard line prepared with purified factor Xa.

TFPI Inhibition and ATIII Binding. The inhibition by TFPI was monitored by amidolytic assays in a 96-well microtiter plate format as described (47) with reaction mixtures containing 10 nM activated mutants, 10 nM sTF, and different concentrations (0–600 nM) of TFPI. After incubation of the enzymes and sTF at room temperature for 10 min, TFPI and S2288 (0.5 mM) were added to the reaction mixtures. The change of absorbance was recorded continuously at 37 °C for 90 min and used to calculate the hydrolysis rate for each reaction. The rates in the absence of TFPI were taken as 100%. Calculation of the inhibition constant followed as described (47). Inhibition in the presence of factor Xa was performed by preincubating TFPI (1 μ M) with equal concentrations of bovine Xa at 37 °C for 30 min to form the TFPI–Xa complex. The residual Xa activity was <5% as measured by hydrolysis of Chromozyme tPA. This TFPI–Xa preparation (1–10 nM) was added to the VIIa–TF complex (4 nM) which was formed by preincubation at 37 °C for 15 min in TBS/Ca/PCPS/BSA. After a further 10 min incubation, S2288 was added to 0.5 mM, and the amidolytic activity was monitored continuously at 37 °C for 90 min. Residual activity was determined and presented with values relative to the activity in the absence of inhibitors.

For ATIII experiments, 1 μ M ATIII was incubated with 0.2 μ M activated mutants in the presence of 3 units/mL heparin at 37 °C. Aliquots of the reaction mixtures were withdrawn at timed intervals, stopped by buffers containing 1% SDS, 2 mM EDTA, and 8% glycerol, and subsequently analyzed by SDS–PAGE followed by silver staining. To obtain second-order rate constants, amidolytic assays were performed as described (28, 48). VIIa (40 nM) was incubated with relipidated TF (40 nM, containing 0.25 mM PCPS) at 37 °C for 20 min in TBS/Ca/BSA. Different concentrations of ATIII (55–77 nM), heparin (10 units/mL), and Chromozyme tPA (0.5 mM) were then added to the mixtures to a total volume of 0.1 mL at 37 °C. The change of absorbance at 405 nm was detected continuously by a spectrophotometer equipped with a thermocontroller and microcuvettes (Hitachi U-3000; Hitachi, Japan). Analysis of the data followed the equation: $\ln [A/(A - i)] = kit - \ln [(A_0 - i)/A_0]$ (48), where A is the concentration of free inhibitor at a given time and i is $A_0 - B_0$ (A_0 and B_0 are the initial concentrations of inhibitor and enzyme, respectively). The data were first plotted as $\ln [A/(A - i)]$ vs time, t , and the derived slope was ki , where k was the second-order rate constant obtained from three experiments with different inhibitor concentrations.

Molecular Modeling. Homology models for the three-dimensional structure of VIIa (49) were generated using Homology in InsightII (Molecular Simulations Inc.) as

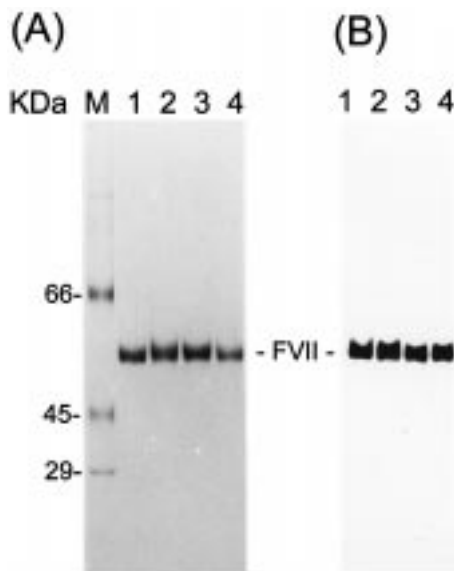


FIGURE 1: SDS-PAGE analysis of VII Q²¹⁷ variants under reducing conditions. Panel A: Silver staining. The amount of purified proteins was 0.3 μ g of protein/lane. Panel B: Western blotting with anti-VII antibody 231-7. Lane M: Molecular weight markers. Lanes 1-4: Recombinant wild-type VII, VIIQ217A, VIIQ217G, and VIIQ217E, respectively.

described (16). The Q²¹⁷ was mutated to A, G, or E, respectively, maintaining side chain orientation in the initial model. Each model was subjected to a short energy minimization followed by 100 ps of molecular dynamics simulation using AMBER 4.1 in a 4 Å shell of water (50).

RESULTS

Effect of Mutation of Q217 on Clotting Activity of VII. Mutants of residue VIIQ²¹⁷ were stably expressed in human 293 cells under the control of the cytomegalovirus promoter. The expression levels were approximately 90 ng/10⁶ cells in 24 h. Purification of the recombinant proteins was facilitated by the use of serum-free media for large-scale culture of the cells. As shown in Figure 1, a single-step QAE-Sephadex column chromatography yielded recombinant VII proteins of high purity and approximately 30% recovery. Determination of their clotting activity by PT assays revealed that VIIQ217E was fully active, VIIQ217A's activity was reduced to 15%, and VIIQ217G had undetectable clotting activity. All the mutant proteins were recognized by several antibodies in ELISA assays and in immunoblotting experiments (Figure 1), indicating that the overall structure of these mutants is not perturbed significantly to account for the loss of coagulation function.

Activation of the Mutants by Factor Xa and the VIIa-TF Complex, and Binding to TF. To examine the biological characteristics of the recombinant proteins, their activation by factor Xa was investigated. As shown in Figure 2, all the proteins were readily activated by factor Xa, and the generated VIIa depicted slower mobility than zymogen VII under nonreducing conditions (panel A). The identities of the activated products have been verified by antibodies under both reducing and nonreducing conditions (not shown). The results suggested that mutation at Q²¹⁷ did not alter the interaction of VII zymogen with factor Xa. When activation of the recombinants by incubation with a limited amount of

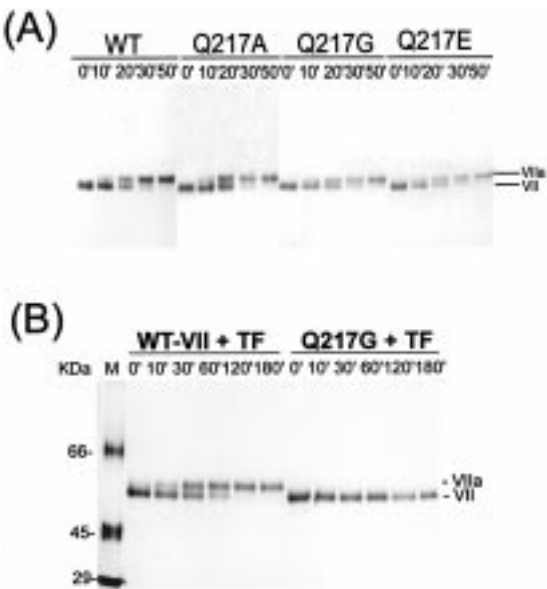


FIGURE 2: Activation of the VII mutants. Panel A: Activation by bovine factor Xa. The enzyme to substrate ratio was 1:500 (w/w). The amount of VII proteins was 0.25 μ g/lane. Time course of activation is indicated above lanes. SDS-PAGE was performed under nonreducing conditions followed by silver staining. Panel B: Autoactivation by adding relipidated TF. Wild-type VII (WT-VII) and VIIQ217G concentrations were 1 μ M, and relipidated TF, 10 nM, and 0.2 μ g of VII(a) were loaded in each lane. The gel condition was as in panel A.

Table 1: TF Binding

zymogen/enzyme	k_{on} ($\times 10^5$ M ⁻¹ s ⁻¹)	k_{off} ($\times 10^{-4}$ s ⁻¹)
VIIwt ^a	3.3 \pm 0.9	7.9 \pm 0.9
VIIQ217A	4.1 \pm 0.3	6.4 \pm 0.6
VIIQ217G	5.9 \pm 0.7	5.3 \pm 0.4
FFR-VIIwt ^b	4.7 \pm 0.7	4.1 \pm 0.6
FFR-VIIQ217A	3.9 \pm 0.6	3.1 \pm 0.7
VIIawt	3.3 \pm 0.1	8.7 \pm 0.4
VIIaQ217G	4.1 \pm 0.2	2.9 \pm 0.5

^a An independent experiment with wild-type VII on different chips gave a k_{on} of 4.2 \pm 0.7 ($\times 10^5$ M⁻¹ s⁻¹) and a k_{off} of 11.4 \pm 1.7 ($\times 10^4$ s⁻¹). ^b The active-site serine was modified by FFR-chloromethyl ketone.

relipidated TF was studied, we found a close correlation of the rate of VII generation with their clotting activities. As an example shown in panel B, while wild-type VIIa was detected after 10 min incubation, VIIQ217G did not show activation after a 3 h incubation. Even at equal molar concentrations of the recombinant proteins and TF (50 nM each), still no activation of VIIQ217G was detected.

To test whether binding of the mutants to TF was impaired, the mutants were tested as competitors for wild-type VII in a plasma clotting assay. As expected from the clotting activities, VIIQ217E did not prolong the clotting time of human plasma, whereas VIIQ217A slightly delayed clotting as compared to identical concentrations of wild-type VII (Figure 3). VIIQ217G was a potent inhibitor of TF-induced coagulation, further indicating normal binding affinity to TF. Direct binding of the mutants to TF was summarized in Table 1. Activated VIIQ217A also bound to TF with similar kinetics as wild-type VIIa. Since the mutation was generated close to the catalytic cleft, we also analyzed the effect of binding of covalent active-site inhibitors on TF interaction. Modification of VIIaQ217A with FFR-chloromethyl ketone increased its affinity for TF to the same level as the wild-

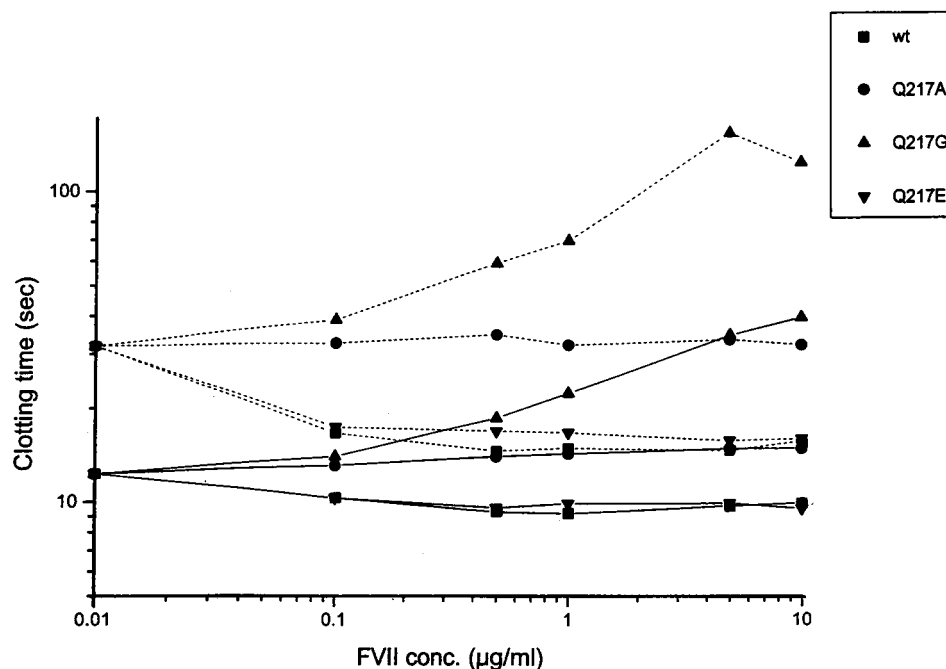


FIGURE 3: Effect of Q²¹⁷ mutants on PT. Clotting times of normal human plasma supplemented with the indicated concentrations of wild-type and mutant recombinant VII were determined as described under Experimental Procedures. Thromboplastin from two different sources was used. Solid lines, human placental thromboplastin. Dashed lines, bovine thromboplastin.

Table 2: Kinetic Values for Factor Xa Generation^a

enzyme	K_M (μM)	V_{max} (nM FXa/min)	k_{cat} (s^{-1})	k_{cat}/K_M ($M^{-1} s^{-1} \times 10^7$)
WT-VIIa	0.29 ± 0.02	103 ± 2.45	5.70	1.91
VIIaQ217E	0.25 ± 0.01	108 ± 11.05	5.98	2.40
VIIaQ217A	0.27 ± 0.01	76 ± 1.17	4.25	1.57
VIIaQ217G	0.40 ± 0.06	4 ± 0.22	0.22	0.05

^a Mean \pm standard deviation, $n = 3$.

type VIIa (Table 1). Thus, mutation of Q²¹⁷ has no effect on any aspect of the VIIa protease domain with the cofactor TF.

Catalytic Activities toward Factors IX and X, and Small Chromogenic Substrates. To address the cause for the loss of clotting activity of the mutants, activation of macromolecular substrates, factors IX and X, was examined. Figure 4 shows that VIIaQ217E activated both proteins comparably to the wild-type VIIa, whereas, VIIaQ217A cleaved both substrates with slightly reduced rates and VIIaQ217G did not show any activities. The kinetics for factor X activation are shown in panel C, for Xa generation in the absence of TF, and in Table 2, for in the presence of TF. In the absence of TF, all the activated recombinants exhibited similar K_M values but different k_{cat} values. Wild-type VIIa and VIIaQ217E showed a k_{cat} value of 0.014 – 0.016 min^{-1} . A nearly 5-fold and 10-fold reduction was obtained with VIIaQ217A and VIIaQ217G, respectively. When TF was present, all recombinants exhibited similar affinities for factor X with a K_M of approximately 0.2 – $0.4 \mu M$. The k_{cat} of VIIaQ217G was reduced drastically but was little impaired for VIIaQ217A and VIIaQ217E. These data clearly demonstrate that the clotting defect of the Q to G mutation is a result of diminished substrate activation. To elucidate the effect of the mutations on small substrate hydrolysis, kinetic parameters for several synthetic substrates were determined in the presence of soluble TF. VIIaQ217G had very low amidolytic

activity. The only substrates that were cleaved with appreciable rates were Chromozyme tPA (Table 3) and Z-Arg-ONb (not shown). VIIaQ217A had k_{cat} values equal to the wild-type VIIa for most substrates. The overall catalytic efficiency for VIIaQ217A was, however, reduced 2–3-fold due to an increased K_M . These data indicate that the mutation has an effect on substrate binding to the catalytic cleft. The K_M for cleavage of most substrates by VIIaQ217E changes little. The k_{cat} increased significantly, most notably for S2765. This may indicate that the Q to E mutation influences aspects of catalysis other than primary substrate binding. These effects may also be of relevance for the drastically reduced function of the Q217G mutant.

TFPI Inhibition and Antithrombin III Binding. The effect of mutation at Q²¹⁷ on the interaction with inhibitors TFPI and ATIII was assessed. Figure 5 shows inhibition by TFPI. TFPI inhibited the amidolytic activity of both VIIaQ217E and VIIaQ217G similar to wild-type VIIa. In contrast, VIIaQ217A was inhibited poorly at low concentrations of TFPI, and a clear difference with the wild-type VIIa persisted in the presence of high concentrations of TFPI. When TFPI was preincubated with VIIa–TF, VIIaQ217A was inhibited to the same extent as wild-type VIIa. The interaction was also examined in the presence of factor Xa (Figure 5, inset). At 2 nM TFPI–Xa complex, the wild-type VIIa's amidolytic activity (in complex with TF) was decreased to 40% of that in the absence of the inhibitor complex, and further reduced to <5% at 5 nM TFPI–Xa. The residual activity of VIIaQ217A was 85% and 65% at 2 nM TFPI–Xa and 5 nM TFPI–Xa, respectively. These data demonstrate that VIIaQ217A is defective in forming an inhibitor complex with the first Kunitz-domain of TFPI.

The interaction of ATIII with the mutants was investigated in the absence (Figure 6A) and presence (Figure 6B) of TF. Figure 6A shows the formation of SDS-stable complexes of mutant and wild-type VIIa with ATIII. Complex formation

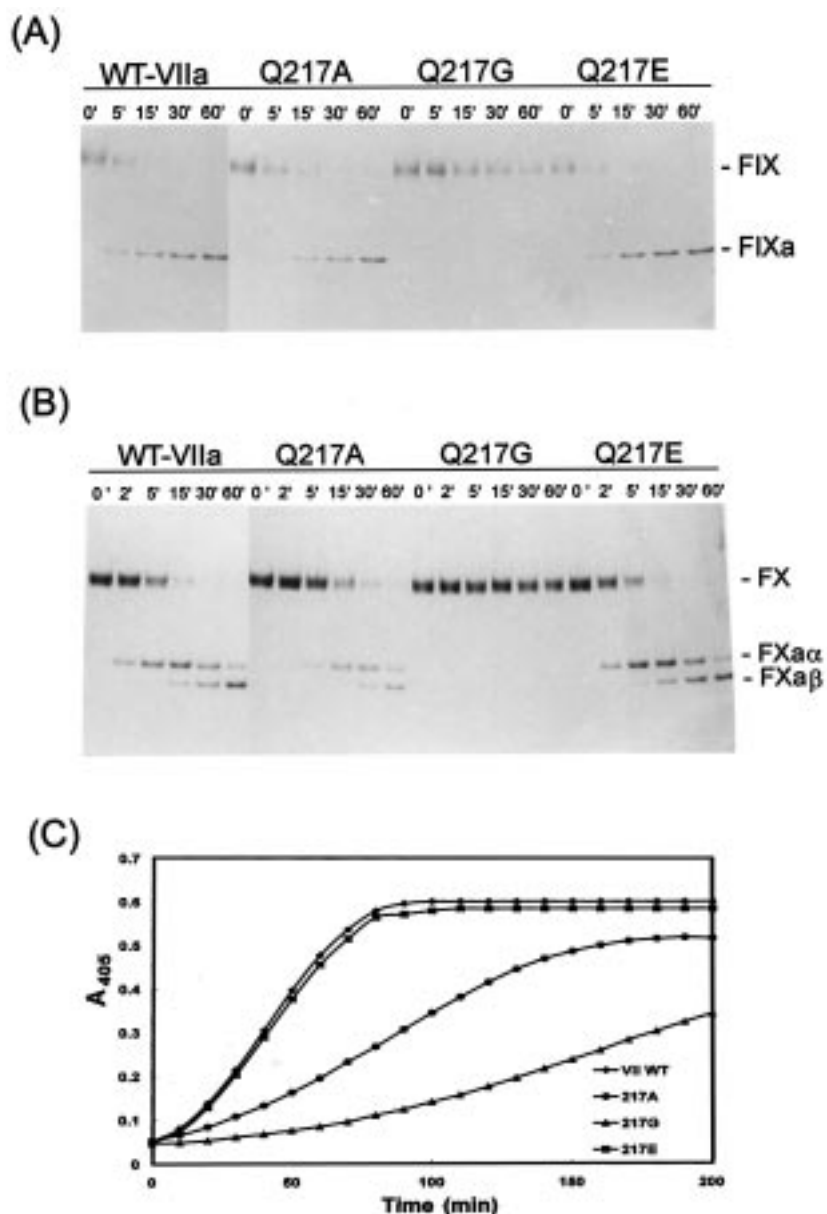


FIGURE 4: Interaction with macromolecular substrates. Panel A: Activation of factor IX. The reactions contained 5 nM VIIa, 6 nM replipidated TF, 200 μ M PCPS, and 0.5 μ M factor IX, and were carried out for the indicated times at 37 °C in TBS/Ca. Products were analyzed by SDS-PAGE under nonreducing conditions and visualized by silver staining. Panel B: Activation of factor X. The final concentrations of the components were as follows: VIIa, 2 nM; replipidated TF, 3 nM; PCPS, 100 μ M; and factor X, 0.4 μ M. Other experimental conditions were as described in panel A. Panel C: Kinetics of Xa generation in the absence of TF. Different concentrations of factor X (0–4 μ M) were used to derive kinetic parameters (as described under Experimental Procedures). Only the data of 1 μ M factor X were depicted. The kinetic values were K_M (μ M) 2.4 ± 0.5 for wild-type VIIa, 2.8 ± 0.7 for VIIaQ217E, and 4.4 ± 0.9 and 4.0 ± 0.5 for VIIaQ217A and VIIaQ217G, respectively. The V_{max} (min^{-1}) was 0.27 ± 0.04 for wild-type VIIa, 0.32 ± 0.09 for VIIaQ217E, 0.06 ± 0.01 for VIIaQ217A, and 0.03 ± 0.004 for VIIaQ217G.

of VIIaQ217A with ATIII appeared slightly more efficient than that of the wild-type VIIa, whereas complex formation of ATIII with VIIaQ217E occurred at lower rates. VIIaQ217G did not form detectable complexes with 0.2 μ M ATIII, and a complex could be detected only at high concentrations (data not shown). The interaction of ATIII with the mutants was also determined by the loss of the amidolytic function of the TF–VIIa complex (panel B). The second-order rate constants were $2.31 \times 10^3 \text{ M}^{-1} \text{ min}^{-1}$ for VIIaQ217A and $0.47 \times 10^3 \text{ M}^{-1} \text{ min}^{-1}$ for VIIaQ217E, as compared with $1.47 \times 10^3 \text{ M}^{-1} \text{ min}^{-1}$ for wild-type VIIa. The low activity of VIIaQ217G did not allow accurate determination of rate constants. These data are consistent with the formation of SDS-stable complexes in the absence of TF.

DISCUSSION

We have generated VII mutants by replacing residue Q²¹⁷, which is typically a conserved E residue in other vitamin K-dependent coagulation factors. Replacement with E, A, and G was done to understand the importance of negative charge and the size of the side chain, and the role of the backbone structure. The three mutants, VIIQ217E, VIIQ217A, and VIIQ217G, demonstrated various degrees of reduction in clotting activities that closely correlated with their in vitro catalytic activity toward factor IX and factor X. This suggests that mutations at Q²¹⁷ affect catalytic activity without altering the substrate selectivity for factors IX and X. VIIQ217E had normal clotting activity. Since E is present in bovine, rabbit,

Table 3: Kinetic Parameters^a

substrates	enzymes			
	WT-VII	Q217E	Q217A	Q217G
Chromozyme t-PA ^b	9.46	10.96	3.51	0.29
(MeSO ₂ -D-Phe-Gly-Arg-pNA)	(5.3 ± 0.03/0.56 ± 0.14)	(16.0 ± 0.70/1.46 ± 0.30)	(7.33 ± 0.47/2.09 ± 0.23)	(0.86 ± 0.68/3.0 ± 0.35)
S-2288	5.47	11.12	2.23	ND ^c
(D-Ile-Pro-Arg-pNA)	(6.35 ± 1.54/1.16 ± 0.28)	(14.23 ± 1.20/1.28 ± 0.08)	(5.98 ± 0.80/2.68 ± 0.50)	
spectrozyme FXa	1.23	2.0	0.35	ND
(MeO-CO-D-chGly-Gly-Arg-pNA)	(2.42 ± 0.90/1.96 ± 0.40)	(3.30 ± 0.85/1.60 ± 0.40)	(2.27 ± 1.50/6.43 ± 0.80)	
S2765	0.66	5.46	0.33	ND
(Z-D-Arg-Gly-Arg-pNA)	(0.43 ± 0.10/0.66 ± 0.15)	(13.77 ± 0.50/2.52 ± 0.50)	(0.13 ± 0.50/0.39 ± 0.14)	

^a Shown are the k_{cat}/K_M (mM⁻¹ s⁻¹) values. Individual k_{cat} (s⁻¹) and respective K_M (mM) are shown in parentheses as the numerator (former) and the denominator (latter). ^b MeSO₂, *N*-methylsulfonyl; Me-CO-, *N*-methoxycarbonyl; Z, *N*-benzyloxycarbonyl. ND: not determined.

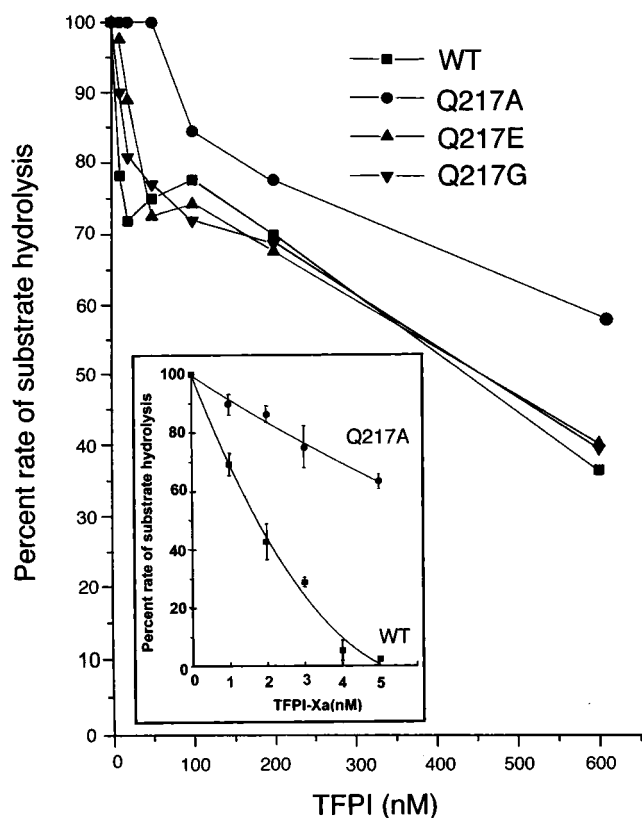


FIGURE 5: TFPI inhibition of mutant and wild-type VIIa. The final concentrations were as follows: VIIa, 10 nM; sTF, 10 nM; TFPI, 0–600 nM; S2288, 0.5 mM. TFPI was added last to the reaction, and the rates of hydrolysis were determined immediately and continued for 90 min. Only curves representing the linear phase of hydrolysis were used for calculation. Residual activities relative to the absence of inhibitor are shown. Means of multiple experiments were plotted. Preincubation of VIIa–TF complex with TFPI was performed for wild-type and VIIaQ217A. The inset depicts the inhibition by TFPI in complex with bovine Xa under the experimental conditions described under Experimental Procedures.

canine, rat, and mouse VII whereas primate VII contains Q, the normal function of VIIQ217E indicates that the side chain characteristics, rather than the charge properties, are relevant for the function of this residue. This notion is supported by the finding that VIIaQ217A exhibited decreased activation of macromolecular and small synthetic substrates without changing the substrate preferences found for wild-type VIIa. However, VIIaQ217E showed enhanced activation of small chromogenic substrates, with higher k_{cat} 's for each of the substrates analyzed.

There are a few possible explanations for the effect of the mutations on the enzymatic activity. First, residues 214–

216 form the bottom of the catalytic cleft, and mutation of Q217 likely affects the substrate binding pocket, in particular the P3 position. Previously, the mutational effects at 397 in factor IX were proposed to reduce the k_{cat} through a structural change at the P3 recognition site, corresponding to residues 215–216 (50). VIIaQ217G showed predominant changes in the k_{cat} rather in the K_M of cleaving factor X, consistent with a decreased rate of scissile bond cleavage. Even though residue 217 is adjacent to the P3 binding site, its side chain is partially buried, and, therefore, the side chain is unlikely to make direct contacts with substrates. This may result in more extended effects on the overall conformation of the catalytic cleft. This second possibility may particularly hold for the significant loss of activity upon G replacement. VIIQ217G was secreted into the cultured media and accumulated to a similar level as the other variants. It could also be activated by bovine factor Xa and interact with TF. Therefore, the G substitution is not likely to cause global structural changes, but rather changes in a local area. To gain further insight to the putative structural changes of each mutation, these proteins have been subjected to molecular dynamics simulations. Shown in Figure 7 are structures after 100 ps. In VIIaQ217G, the backbone of residues 215–218 (in blue) shifted toward the active-site serine relative to that in wild-type VIIa. These changes likely reflect increased flexibility introduced by the series of G residues. The modeling also indicated a smaller opening for approach to the active site and some new hydrogen bonds within the pocket. Taken together, these changes may explain the failure of VIIaQ217G to effectively hydrolyze substrates. We also observed a shift in the backbone position at the P3 binding site (in blue) in VIIaQ217A relative to the active-site pocket, although to a less extent. In VIIaQ217E, the backbone structure as well as the position of the side chain of 217 were very similar to the structure of wild-type VIIa.

The crystal structure of the factor VIIa–TF complex revealed that residue 217 is distant from the TF binding sites. It is also distant from the loop of a charged surface region (around residue 168) proposed to be the heparin binding site in the thrombin–ATIII complex. However, some hydrogen bonds were observed between part of the loop and the side chain of residue 217 in both the thrombin (threonine at 172) and factor Xa (serine at 173) crystal structures. The 2–3-fold differences in ATIII inhibition rate with VIIaQ217A and VIIaQ217E may be mediated by changes in the contact between the loop and the side chain of 217. The inhibition of factor VIIa by ATIII has recently been suggested to be another physiological regulator of factor VIIa–TF-dependent

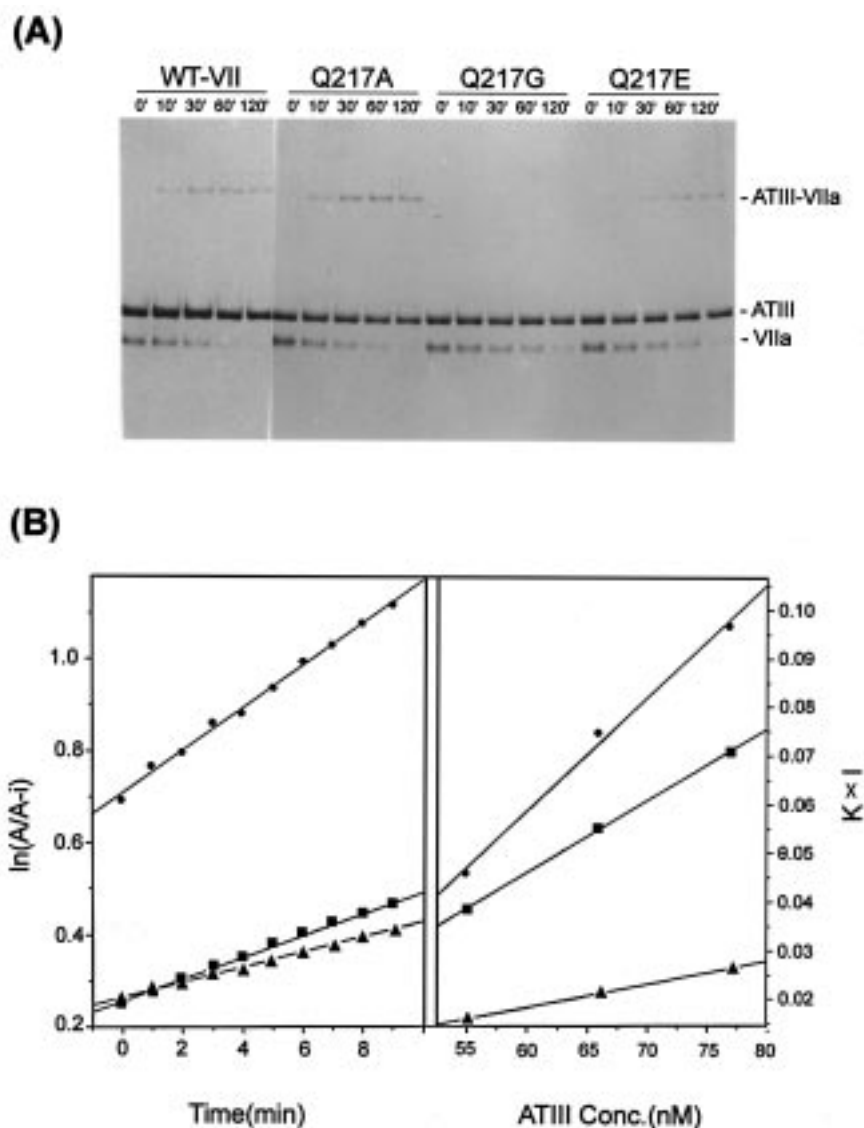


FIGURE 6: Interaction of wild-type and mutant VIIa with ATIII. Panel A: Wild-type VIIa (WT-VIIa) or the indicated mutants (0.2 μ M) were incubated with ATIII (1 μ M) and heparin (3 units/mL) for the indicated times followed by quenching with nonreducing SDS-PAGE sample buffer. The amount of VIIa in each lane was 0.18 μ g. Panel B: Inhibition of amidolytic activity was analyzed by forming the TF-VIIa complex (40 nM each) followed by the addition of ATIII, heparin, and Chromozyme tPA. Circles, VIIaQ217A; squares, wild-type VIIa (WT-VIIa); triangles, VIIaQ217E. The ATIII concentration used in the left column was 55 nM. I is identical to i , the initial concentration of the inhibitor (A_0) subtracted from the concentration of the enzyme (B_0) as described by Downing et al. (48).

coagulation (27, 28, 30). Since the inhibition has been proposed to proceed through the recognition of the R³⁹³–S³⁹⁴ bond in an exposed loop of ATIII as a substrate, the lack of complex formation between VIIaQ217G and ATIII may be due to the proposed changes in the primary specificity pocket. Surprisingly, we observed the more effective binding of VIIaQ217A to ATIII, whereas the same mutation in thrombin (thrombin E229A) resulted in less effective binding (35). Moreover, VIIaQ217E was less interactive with ATIII, despite having normal enzymatic activity toward factors IX, X, and VII. Taken together, this may indicate that mutation of Q²¹⁷ induces subtle changes in the catalytic cleft, rather than eliminates specific side chain interactions with the reactive loop of the inhibitor ATIII. In terms of inhibition by TFPI, the effect of mutations at 217 was much less pronounced compared with the reported effect of the mutations at 192 (47, 51, and unpublished results). Only VIIaQ217A exhibited slightly reduced inhibition by TFPI alone and by the TFPI–Xa complex.

Factor VII is an attractive protein for its therapeutic potential. It is quite stable and easy to be engineered for mass production (6). Clinical findings suggested that VII(a) is a hemostatic risk factor for thrombosis in Caucasian (52) and in Chinese (unpublished results). Moreover, the TF pathway is also the major activator of coagulation in various pathological states, including Gram-negative sepsis, atherosclerosis, and tumor metastasis (53–55). Mutants of Q²¹⁷s may provide different opportunities for therapies, and detailed characterization of their biochemical properties should provide significant information in this regard.

ACKNOWLEDGMENT

We thank Dr. Yiu Shou-Yin at the Department of Pharmacy for providing facilities for the preparation of PCPS and Ms. Pai-Chih Wu, Mr. Chia-Chen Lee, and Mr. Hsiang-Ming Wang for technical assistance. We also thank Dr. Paul Clarifson and Drs. Li-Tzu Li and Ying-Shuan E. Lee for helpful discussions.

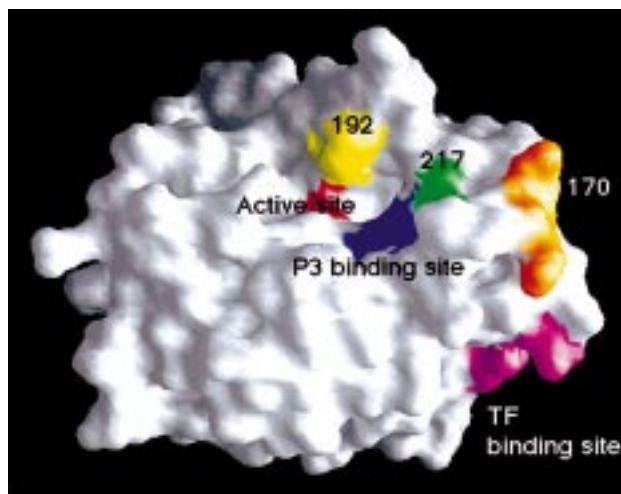


FIGURE 7: GRASP surface presentation of the factor VII catalytic domain (DAN.PDB). The active-site serine is shown in red. Residues 217, 192, and 170C-D are shown in green, yellow, and orange, respectively. Also shown in blue is the P3 binding site (residues 215–216). Part of the TF binding site is shown in pink. The rest of the TF binding sites are extended to the back of the molecule.

REFERENCES

- Davie, E. W., Fujikawa, K., and Kisiel, W. (1991) *Biochemistry* 30, 10363–10370.
- Hagen, F. S., Gray, C. L., O'Hara, P., Grant, F. J., Saari, G. C., Woodbury, R. G., Hart, C. E., Insley, M., Kisiel, W., Kurachi, K., and Davie, E. W. (1986) *Proc. Natl. Acad. Sci. U.S.A.* 83, 2412–2416.
- O'Hara, P. J., Grant, F. J., Haldeman, B. A., Gray, C. L., Insley, G. M., Hagen, F. S., and Murry, M. J. (1987) *Proc. Natl. Acad. Sci. U.S.A.* 84, 5158–5162.
- Rao, L. V. M., and Rapaport, S. I. (1988a) *Blood* 72, 396–401.
- Radcliffe, R., and Nemerson, Y. (1976) *J. Biol. Chem.* 251, 4797–4802.
- Seligsohn, U., Kasper, C. K., Osterud, B., and Rapaport, S. I. (1979) *Blood* 53, 828.
- Wildgoose, P., and Kisiel, W. (1989) *Blood* 73, 1888–1895.
- Kisiel, W., Fujikawa, K., and Davie, E. W. (1977) *Biochemistry* 16, 4189–4194.
- Broze, G. J., Jr., and Majerus, P. W. (1980) *Methods Enzymol.* 80, 228–237.
- Nagakaki, T., Foster, D. C., Berkner, K. L., and Kisiel, W. (1991) *Biochemistry* 30, 10819–10824.
- Yamamoto, M., Nakagaki, T., and Kisiel, W. (1992) *J. Biol. Chem.* 267, 19089–19094.
- Nemerson, Y., and Esnouf, M. P. (1973) *Proc. Natl. Acad. Sci. U.S.A.* 70, 310–314.
- Lawson, J. H., Butenas, S., and Mann, K. G. (1992) *J. Biol. Chem.* 267, 6375–6381.
- Ruf, W., Rehemtulla, A., and Edgington, T. S. (1991) *J. Biol. Chem.* 266, 2158–2166.
- Ruf, W. (1994) *Biochemistry* 33, 11631–11636.
- Dickinson, C. D., Kelly, C. R., and Ruf, W. (1996) *Proc. Natl. Acad. Sci. U.S.A.* 93, 14379–14384.
- Ruf, W., Kelly, C. R., Schullek, J. R., Martin, D. M. A., Polikarpov, I., Boys, C. W. G., Tuddenham, E. G. D., and Edgington, T. S. (1995) *Biochemistry* 34, 6310–6315.
- Banner, D. W., D'Arcy, A., Chene, C., Winkler, F. K., Guha, A., Konigsberg, W. H., Nemerson, Y., and Kirchhofer, D. (1996) *Nature* 380, 41–46.
- Seligsohn, U., Kasper, C. K., Osteiud, B., and Rapaport, S. I. (1979) *Blood* 53, 828–837.
- Bauer, K. A., Kass, B. L., ten Cate, H., Hawiger, J. J., and Rosenberg, R. D. (1990) *Blood* 87, 731–736.
- Girard, T. J., Warren, L. A., Novotny, W. F., Likert, K. M., Brown, S., Miletich, J. P., and Broze, G. J., Jr. (1989) *Nature* 338, 518–520.
- Broze, G. J., Jr., and Miletich, J. P. (1987) *Blood* 69, 150–155.
- Rapaport, S. I. (1991) *Thromb. Haemostasis* 66, 6–15.
- Gammel, C. H., Broze, G. J., Turitto, V. T., and Nemerson, Y. (1990) *Blood* 79, 2266–2271.
- Pederson, A. H., Nordfang, O., Norris, F., Wiberg, F. C., Christensen, P. M., Moeller, K. B., Meidahl-Pederson, J., Beck, T. C., Norris, K., Hedner, U., and Kisiel, W. (1990) *J. Biol. Chem.* 265, 16786–16793.
- Callander, N. S., Rao, L. V. M., Nordfang, O., Sandset, P. M., Warn-Cramer, B., and Rapaport, S. I. (1992) *J. Biol. Chem.* 267, 876–882.
- Kondo, S., and Kisiel, W. (1987) *Thromb. Res.* 46, 325–335.
- Lawson, J. H., Butenas, S., Ribarik, N., and Mann, K. G. (1993) *J. Biol. Chem.* 268, 767–770.
- Broze, G. J., Jr., Likert, K., and Higuchi, D. (1993) *Blood* 82, 1679–1680.
- Bjorquist, P., and Bostrom, S. (1997) *Thromb. Res.* 85, 225–236.
- Hedner, U. (1990) *Blood Coagulation Fibrinolysis* 1, 307–317.
- Tsiang, M., Jain, A. K., Dunn, K. E., Rojas, M. E., Leung, L. L. K., and Gibbs, C. S. (1995) *J. Biol. Chem.* 270, 16854–16863.
- Gibbs, C. S., Coutre, S. E., Tsiang, M., Li, W.-X., Jain, A. K., Dunn, K. E., Law, V. S., Mao, C. T., Matsumura, S. Y., Mejza, S. J., Paborsky, L. R., and Leung, L. L. K. (1995) *Nature* 378, 413–416.
- Tsiang, M., Jain, A. K., and Gibbs, C. S. (1997) *J. Biol. Chem.* 272, 12024–12029.
- Crem, M. M., and Di Cera, E. (1998) *Proteins: Struct., Funct., Genet.* 30, 34–42.
- Stone, M. J., Ruf, W., Miles, D. J., Edgington, T. S., and Wright, P. E. (1995) *Biochem. J.* 310, 605–614.
- Higashi, S., Nishimura, H., Fujii, S., Takada, K., and Iwanaga, S. (1992) *J. Biol. Chem.* 267, 17990–17996.
- Cerskus, A. L., Ofofu, F. A., Clarke, B. J., Modi, G. J., Johnston, M., and Blajchman, M. A. (1985) *Br. J. Haematol.* 61, 467–475.
- Lin, S. W., Lin, S. R., and Shen, M. C. (1993) *Genomics* 18, 496–504.
- Lin, S. W., Smith, K. J., Welch, D., and Stafford, D. W. (1990) *J. Biol. Chem.* 265, 144–150.
- Thomsen, D. R., Stenberg, R. M., Goins, W. F., and Stinski, M. F. (1984) *Proc. Natl. Acad. Sci. U.S.A.* 84, 4767–4771.
- Bradford, M. (1976) *Anal. Biochem.* 72, 248.
- Szoka, F., and Papahadjopoulos, D. (1978) *Proc. Natl. Acad. Sci. U.S.A.* 75, 4194–4198.
- Stewart, J. C. M. (1980) *Anal. Chem.* 104, 10–14.
- Zhong, D., Smith, K. J., Birktoft, J. J., and Bajaj, S. P. (1994) *Proc. Natl. Acad. Sci. U.S.A.* 91, 3574–3578.
- Fiore, M. M., Neuenschwander, P. F., and Morrissey, J. H. (1992) *Blood* 80, 3127–3134.
- Neuenschwander, P. F., and Morrissey, J. H. (1995) *Biochemistry* 34, 8701–8707.
- Downing, M. R., Bloom, J. W., and Mann, K. G. (1978) *Biochemistry* 17, 2649–2653.
- Banner, D. W., D'Arcy, A., Chene, C., Winkler, F. K., Guha, A., Konigsberg, W. H., Nemerson, Y., and Kirchhofer, D. (1996) *Nature* 380, 41–46.
- Hamaguchi, N., Charifson, P. S., Pedersen, L. G., Brayer, G. D., Smith, K. J., and Stafford, D. W. (1991) *J. Biol. Chem.* 266, 15213–15220.
- Chang, S. C., Lu, T. T., Ruf, W., Shen, M. C., and Lin, S. W. (1995) *Thromb. Haemostasis* 73, 1165a.
- Ridker, P. M. (1997) *Thromb. Haemostasis* 78, 53–59.
- Niemetz, J., and Morrison, C. (1977) *Blood* 49, 947–956.
- Wilcox, J., Smith, K., Schwartz, S., and Gordon, D. (1989) *Proc. Natl. Acad. Sci. U.S.A.* 86, 2839–2843.
- Donati, M. B. (1995) *Thromb. Haemostasis* 74, 278–281.